



Nonlinear analysis of compensated asymmetric energy harvester

João Pedro Norenberg¹, Roberto Luo², Vinicius Lopes², João Victor Peterson² and Americo Cunha Jr²

¹ São Paulo State University – UNESP, Ilha Solteira - SP, Brazil

² Rio de Janeiro State University – UERJ, Rio de Janeiro - RJ, Brazil

Abstract: Nonlinear vibration energy harvesting can convert kinetic energy into electricity at a broadband frequency. However, asymmetries can arise during a manufacturing process and drastically impair energy generation. Therefore, this work numerically investigates the effect of asymmetry on a bistable energy harvester using the bifurcation diagram and the basins of attractions proposed based on tests 0-1 for chaos. We introduce the asymmetries using a quadratic term on the restoring force and an external force due to the slope angle of the plane where the system is attached. A particular condition is established that an asymmetric term compensates the effect of the other one. The results indicated that although the asymmetric conditions the dynamic behavior becomes symmetric, and the negative effect of asymmetry can be avoided, enhancing the energy harvesting process.

Keywords: vibration energy harvesting, nonlinear dynamics, bistable oscillator, asymmetries, basins of attraction

INTRODUCTION

Energy harvesting can be an essential technique to provide greater autonomy to electronic mobile devices. It consists of converting available energy sources in the environment such as vibration, heat, and wind into electricity. This technology proved to be promising in low-energy demand applications, e.g., sensors, actuators, pacemakers, and IoT devices. Several recent works have been developed in different applications.

Among commonly available energy sources present in the environment, the vibration source from environmental and structural noise has been explored for harvesting energy. Linear vibration energy harvesting devices, despite their dynamic simplicity, typically provide reduced output power in regions away from the resonance. To overcome this limitation, Cottone, Vocca, and Gammaitoni (2009) and Erturk, Hoffmann, and Inman (2009) proposed nonlinear systems to potentially increase the frequency bandwidth.

Numerous efforts have been dedicated to bistable energy harvesters proposed by Erturk, Hoffmann, and Inman (2009). They built a piezo-magnetic-elastic system. Several works suppose a perfectly symmetric system, but it is arduous to fabricate it mainly because, in most cases, the asymmetries are unavoidable, for instance, from the geometry, physical properties, mechanical loads, and magnetic fields. Recently, Cao et al. (2015) and Wang et al. (2018a) assessed the asymmetry effect of a bistable energy harvester. They verified that asymmetries are prejudicial to harvesting performance, decreasing the energy output compared to a symmetrical system. They also visualized that the dynamic becomes more complex because one more nonlinearity appeared.

This work investigates the dynamic behavior of asymmetric bistable energy harvesting systems. We calculate the bifurcation diagrams to study the multiple solutions sweeping the amplitude and frequency of excitation. The basins of attraction based on Test 0-1 for chaos proposed by Norenberg et al. (2022b) are also calculated to examine the incidence of chaotic behavior concerning the initial conditions. Using these classical nonlinear tools, we conduct a comprehensive study of asymmetric bistable energy harvesters and compare them to the symmetric model. A particular condition of the asymmetric model is established and studied to compensate the asymmetric effect.

ASYMMETRIC PIEZO-MAGNETO-ELASTIC ENERGY HARVESTER

Figure 1 illustrates the asymmetric bistable piezo-magneto-elastic energy harvester proposed by Norenberg et al. (2022a). This system consists of a vertical clamped-free ferromagnetic beam. The beam is fixed at a rigid base where a pair of magnets is placed on the lower part. Two piezoelectric layers are placed on the beam's highest part, the region of higher deformation. The rigid base is periodically excited by an external source. When this motion deforms the piezoelectric layers, the kinetic energy of vibration is converted into electricity and is dissipated in the resistor. In order to introduce the asymmetric features, the harvester is attached to a plane with a sloping angle ϕ , arising an external force due to gravitational effect, and we also assume that the magnets are not identical, inducing asymmetric potential energy. Taking into account these features, we obtain a sophisticated model. The system is perfectly symmetric when we neglect these features.

The following dimensionless initial value problem describes the governing lumped-parameter equation of motion of the asymmetric piezo-magneto-elastic energy harvester

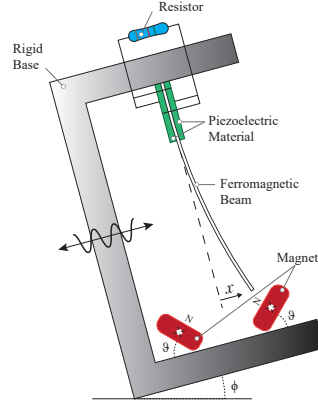


Figure 1: Illustration of the asymmetric piezo-magneto-elastic energy harvester.

$$\ddot{x} + 2\xi\dot{x} - \frac{1}{2}x(1 + 2\delta x - x^2) - \chi v = f \cos(\Omega t) + p \sin(\phi), \quad (1)$$

$$\dot{v} + \lambda v + \kappa \dot{x} = 0, \quad (2)$$

$$x(0) = x_0, \dot{x}(0) = \dot{x}_0, v(0) = v_0, \quad (3)$$

where t denotes time; x is the beam tip amplitude of oscillation; v is the voltage in the resistor; ξ is the damping ratio; f is the rigid base oscillation amplitude; Ω is the external excitation frequency; λ is a reciprocal time constant; the piezoelectric coupling terms are represented by χ , in the mechanical equation, and by κ in the electrical one; δ is a coefficient of the quadratic nonlinearity (asymmetry of not identical magnets), p is the equivalent gravity of ferromagnetic beam, and ϕ is the sloping angle; x_0 represents the beam edge initial position; \dot{x}_0 is the beam edge initial velocity; and v_0 denotes the initial voltage over the resistor. The upper dot is an abbreviation for time derivative. These parameters are all dimensionless.

Compensation of the asymmetric effects

In order to compensate the asymmetry configurations and obtain a symmetric model, the sum of the nonlinear restoring force for the equilibrium point needs to be zero (Wang et al., 2018b), i.e., $F_r(x_1) + F_r(x_2) = -\frac{1}{2}x_1(1 + 2\delta x_1 - x_1^2) - \frac{1}{2}x_2(1 + 2\delta x_2 - x_2^2) - 2p \sin(\phi) = 0$, where x_1 and x_2 are the stable equilibrium points. When this condition is established, the asymmetries compensate themselves, and the system has a symmetric configuration. Therefore, we can calculate the value of the sloping angle (ϕ_{opt}) that cancels the asymmetry of the quadratic coefficient as

$$\phi_{opt} = \arcsin\left(\frac{8\delta^3 + 9\delta}{27p}\right). \quad (4)$$

RESULTS AND DISCUSSION

Numerical simulations are carried out for $\xi = 0.01$, $\chi = 0.05$, $\lambda = 0.05$, $\kappa = 0.5$, and $\delta = 0.15$. The amplitude and frequency of excitation are varied. Three values of the slope angle ϕ are evaluated: (i) $\phi = 0^\circ$, for symmetric condition (in this situation, $\delta = 0$); (ii) $\phi = 35^\circ$, for strong asymmetric condition; (iii) $\phi = -5^\circ$, for the condition of asymmetries compensation (value obtained from Eq. (4) when $\delta = 0.15$). The codes are available on Norenberg et al. (2021).

Bifurcation diagrams

Bifurcation diagrams were plotted, in Fig. 2, sweeping up and down the excitation amplitude and frequency. Sampling analysis intervals for forcing parameters are set as $0.1 \leq \Omega \leq 1.4$ for the frequency and $0.01 \leq f \leq 0.3$ for the amplitude.

The symmetric condition, Fig. 2a, provides a rich behavior regards the chaos and period multiplicity occurrence. The bifurcation diagrams sweeping the amplitude for the asymmetric model when $\phi = 35^\circ$ are shown in Fig. 2b. The chaotic regions disappeared, and the dynamic behavior is periodic for all excitation values with low power energy. For sweeping the frequency of excitation, there are periodic conditions (one or more periods), but the chaos disappeared. The bifurcation diagram for the asymmetric compensation model is shown in Fig. 2c. The dynamic behavior of this condition presented similar to the symmetric case in that the chaos and multiple periodic responses appear in the same forcing conditions.

Basins of attractions

Basins of attraction numerically study the dynamic response for different initial conditions. It indicates where the different attractors can coexist with the underlying dynamical system. This study integrates the dynamics for different

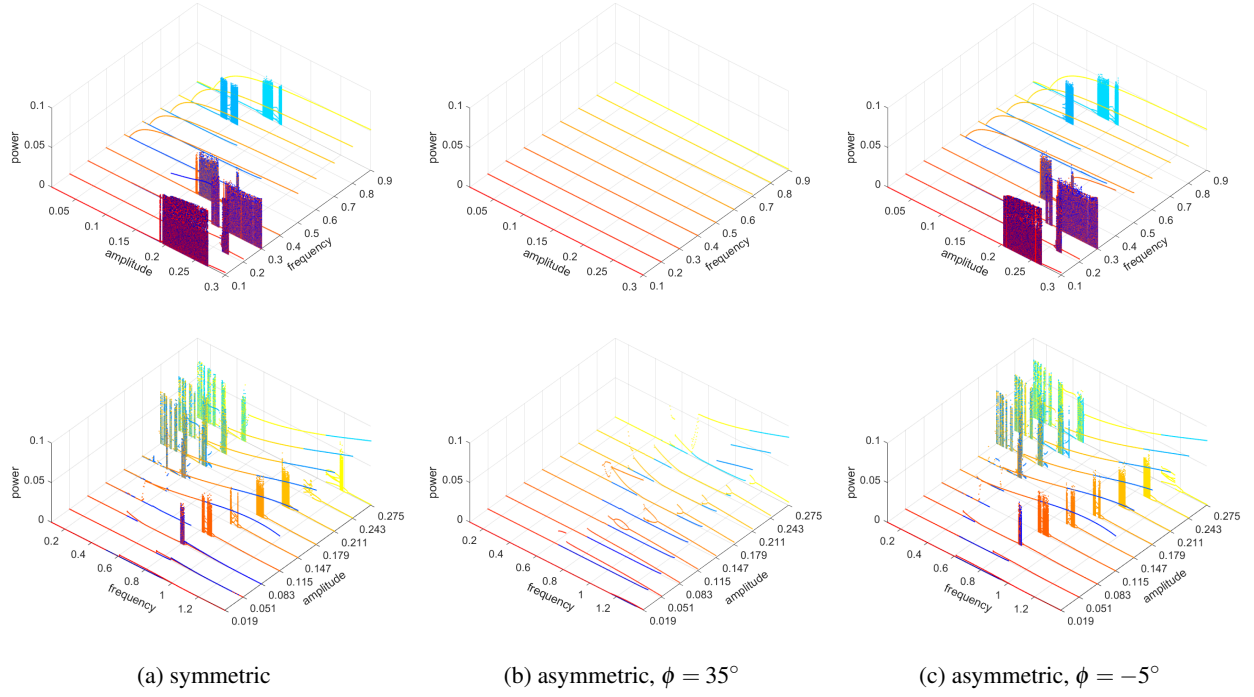


Figure 2: Power bifurcation diagram sweeping forward (blue scale) and backward (red scale) amplitude of excitation (top) and the frequency of excitation (bottom).

sets of initial conditions and maps the possible attractors in which the phase space trajectory can accumulate. The test 0-1 for chaos is used to characterize the dynamics, determining if the system evolves to the chaotic or regular response (Gottwald and Melbourne, 2016). When the test indicates an irregular response, we scheduled to catalog the node with a grey color. When it indicates the regular response, we establish one step to identify the attractors and distinguish the different periodic orbits. The green color is a pattern color to indicate the regular high-energy orbit (cycle limit behavior) that is the best scenario for the harvesting process. The red and blue colors indicate regular low-energy orbits, not appropriate for harvesting energy because the system is monostable. Other colors, e.g., magenta and cyan, indicate regular behaviors but are different energy from red and blue orbits.

Figure 3 displays the basins of attractions when the amplitude of excitation is fixed at $f = 0.019$ and its frequency is fixed at $\Omega = 0.8$. While Fig. 4 displays the basins of attractions for the $f = 0.211$ and $\Omega = 0.8$. The three configurations are presented in each figure. The initial displacement \times initial velocity plane is defined in the region $(x_0, \dot{x}_0) \in [-3 \leq x_0 \leq 3] \times [-3 \leq \dot{x}_0 \leq 3]$ at the restriction plane to $v_0 = 0$.

For the symmetrical and compensated asymmetrical at Fig. 3a and c, respectively, we observed four regular attractors with pulverized regions that express the sensitivity to the initial conditions. However, for the asymmetric model (Fig. 3b), the red basins, low energy attractor, is prevalent throughout the plane, demonstrating the worst scenario for harvesting performance. When the amplitude of excitation increases, $f = 0.211$ (Fig. 4), for the symmetric and compensated asymmetric, the basin is entirely covered by a high energy orbit, demonstrating the desired situation for the energy harvesting process. For the asymmetric model, there are two solutions, green and red basins, but the low-energy solution is dominant. In this situation, we can also visualize that the basins are also asymmetric, such as the well of the right stable equilibrium point is deeper than the left stable equilibrium point.

It is worth mentioning that the basins are symmetric for the compensated asymmetric model. The basins of attractions of the symmetric are similar to the asymmetric, and the solutions presented the same behaviors. Therefore, despite the asymmetric terms added in the model, the asymmetries were compensated, and the system became symmetric.

CONCLUSION

This work numerically investigates the dynamic behavior of the asymmetric bistable energy harvester. Forward and backward bifurcations diagrams of the amplitude and frequency of excitation were plotted to indicate multiple solutions. Basins of attraction based on Test 0-1 were proposed to investigate the attractor projections for different initial conditions. We performed this examination for a strong asymmetric and compensated asymmetric configuration and compared them to the symmetric one. The predominance of low-energy orbits of the asymmetric model was visualized. However, when the external gravitational force canceled the asymmetry of magnets, the system has similar dynamic behavior to the

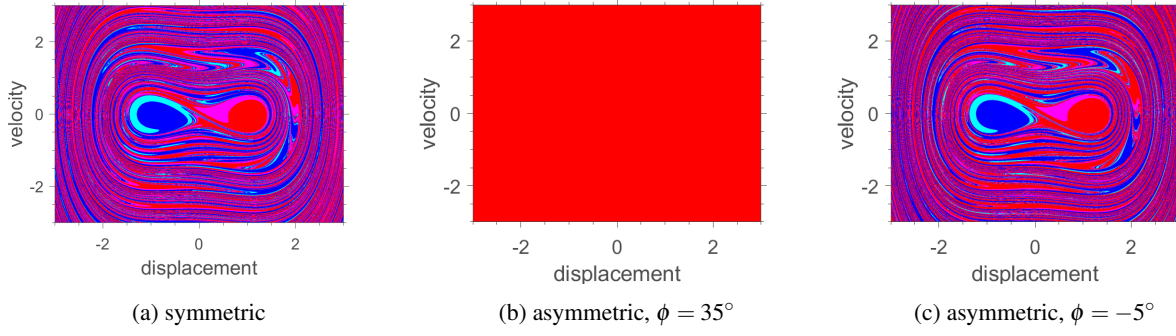


Figure 3: Basins of attraction to the region $\{(x_0, \dot{x}_0) \mid -3 \leq x_0 \leq 3 \text{ and } -3 \leq \dot{x}_0 \leq 3\}$ for $f = 0.019$ and $\Omega = 0.8$.

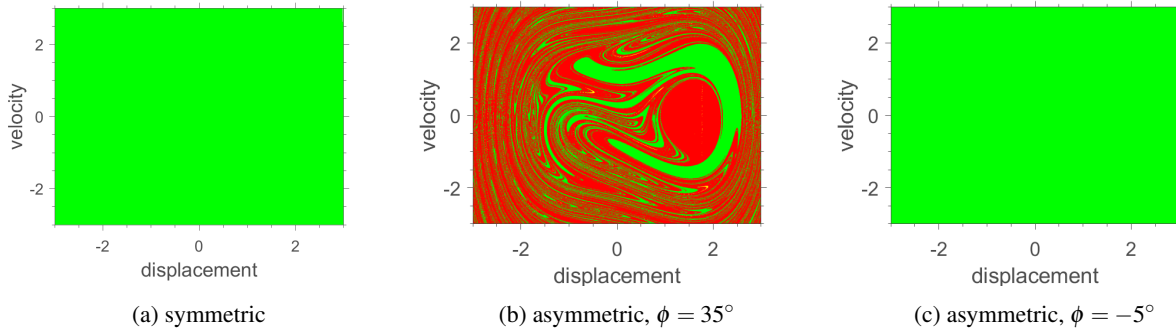


Figure 4: Basins of attraction to the region $\{(x_0, \dot{x}_0) \mid -3 \leq x_0 \leq 3 \text{ and } -3 \leq \dot{x}_0 \leq 3\}$ for $f = 0.211$ and $\Omega = 0.8$.

symmetric bistable, presenting high-energy orbits.

ACKNOWLEDGMENTS

The authors gratefully acknowledge the financial support from CAPES, CNPq, and FAPERJ.

REFERENCES

- Catacuzzano, L., Orfei F., Di Michele, A., Sforza, L., Franciolini, F. and Gammaitoni L., 2019, “Energy harvesting from a bio cell”, *Nano Energy*, Vol.823, pp. 823-827.
- Cottone, F., Vocca, H. and Gammaitoni, L., 2009, “Nonlinear Energy Harvesting”, *Physical Review Letters*, Vol.102, pp. 080601.
- Erturk, A., Hoffmann, J. and Inman, D.J., 2009, “A piezomagnetoelastic structure for broadband vibration energy harvesting”, *Applied Physics Letters*, Vol.94, pp. 254102.
- Gottwald, G.A. and Melbourne, I., 2016, “The 0-1 Test for Chaos: A Review”, *Chaos Detection and Predictability*, Vol.915, pp. 221-247.
- Norenberg, J.P., Cunha Jr, A., da Silva, S., Varoto, P.S., 2022a, “Global sensitivity analysis of asymmetric energy harvesters”, *Nonlinear Dynamics*, Vol.109, pp. 443–458.
- Norenberg, J.P., Peterson, J.V., Lopes, V.G., Luo, R., Roca, L., Pereira, M., Ribeiro, J.G., and Cunha Jr, A., 2021, “STONEHENGE Suite for nonlinear analysis of energy harvesting systems”, *Software Impacts*, Vol.10, pp. 100161.
- Norenberg, J.P., Luo, R., Lopes, V.G., Peterson, J.V., and Cunha Jr, A., 2022b, “Nonlinear dynamic analysis of asymmetric bistable energy harvester”, (*preprint*).
- Wang, W., Cao, J., Bowen, C.R., Inman, D.J. and Lin, J., 2018a, “Performance enhancement of nonlinear asymmetric bistable energy harvesting from harmonic, random and human motion excitations”, *Applied Physics Letters*, Vol.112, pp. 213903.
- Wang, W., Cao, J., Bowen, C.R., Zhang, Y. and Lin, J., 2018b, “Nonlinear dynamics and performance enhancement of asymmetric potential bistable energy harvesters”, *Nonlinear Dynamics*, Vol.94, pp. 1183-1194.

RESPONSIBILITY NOTICE

The authors are the only responsible for the printed material included in this paper.